

Development and Mechanical Characterization of Eco-Friendly Construction Materials Using Industrial Waste: A Sustainable Approach to Reducing Carbon Footprints in Infrastructure Projects

Sanaa Ismael Khaleel*

College of engineering, Salahaddin Univ., Kirkuk Rd., Erbil, Iraq

* Corresponding Author Email: sanaa.khaleel@su.edu.krd - ORCID: 0000-0002-5247-7851

Article Info:

DOI: 10.22399/ijcesen.2249

Received : 23 February

Accepted : 05 May 2025

Keywords

Eco-Friendly Concrete

Industrial Waste

Colloidal Nanosilica

Metakaolin, Alccofine

Sustainability

Cement Replacement

Abstract:

The construction industry needs sustainable concrete options to serve as regular concrete replacements because of high carbon dioxide emissions produced in construction. An study through science addresses industrial waste materials to determine their suitability as supplementary cementitious materials (SCMs) that enhance concrete properties. Results from compressive strength testing of materials ended up combined with workability results and detailed microscopic examination of cement replacement actions through the study. Research analysts conducted physical along with chemical material evaluations through XRD for X-ray diffraction and scanning electron microscopy (SEM) along with FTIR for Fourier transform infrared spectroscopy and TGA for thermogravimetric analysis testing procedures. The research confirmed that concrete exhibited higher strength performance by combining CNS with MK and AF. The research team created pozzolanic methods which improved microvoid strength by enhancing density while concurrently decreasing harmful portlandite crystals. Lab results show that the usage of supplemental cementitious materials improves concrete performance significantly according to ANOVA statistical tests which underwent T-test verification. Supplemental implementation methods provide both strengthened property features and increased service duration yet establish workable measures for decreasing cement production impacts on the environment. Evidence shows that CNS achieves effective reduction of infrastructure carbon emission rates together with MK and AF. A combination of CNS and MK and AF leads to concrete material with its maximum sustainable operational capabilities.

1. Introduction

Driven through rising demand coming from the building sector, and environmental protection organizations, the creation for sustainable, eco-friendly concrete—also known as "green concrete"—has attracted great interest within recent years. Growing focus upon lowering the environmental effect for conventional concrete has spurred significant study upon the use for mineral admixtures, or Supplementing Cementitious Materials (SCMs), as partial substitutes for cement. Derived coming from either natural sources as kaolin, and limestone or coming from industrial by-products, and waste materials such fly ash, silica fume, and slag, these SCMs are The main technical advantages for these materials arise coming from their tiny particle size, and pozzolanic reactivity,

which greatly help to enhance concrete qualities [1].

Widely employed within the building sector, pozzolanic ingredients such silica fume, fly ash, rice husk ash, and slag improve the mechanical qualities, and lifetime for concrete. for the many elements available, slag has shown significant improvements within concrete performance, which has helped to set guidelines for its usage within cement mixes [2]. Özbay et al. (2016) claim, that these components are rather useful for improving the mechanical characteristics for concrete, especially within difficult circumstances as marine, and acidic ones. Although the gradual development for the microstructure within the early phases for concrete curing may lower its resistance to environmental deterioration, the addition for ultra-fine slag, known as Alccofine (AF), has

demonstrated remarkable qualities, enhancing concrete performance within terms for strength, workability, segregation resistance, and durability [3].

Another useful SCM, metakaolin (MK), has drawn much study focus upon account for its strong pozzolanic action. A technique using much less energy than conventional cement manufacture, which usually takes place for around 1400°C, MK is made through calcining kaolin clay for temperatures between 650°C, and 800°C [4]. MK manufacturing is therefore more economical, and energy-efficient than cement manufacturing. Unas other SCMs, MK is a main product: others are by-products or industrial waste. This helps to improve concrete qualities through enabling more regulated production methods to reach desired traits. Research has shown, that MK greatly increases the resistance for concrete to water, chloride, and sulfate penetration, and speeds the hydration process, hence strengthening its strength, and durability [5,6]. Apart coming from these mineral-based additives, the fast development for nanotechnology has created fresh paths for enhancing concrete performance. Researchers have looked for nanomaterials as nanosilica for their effects upon the strength, and transport characteristics for concrete. Studies have shown, that nanosilica improves cement hydration through offering more nucleation sites for the development for hydration products due for its tiny particle size, and large surface area. Concrete made alongside nanosilica is thus stronger, more durable, and more microstructurally interesting than, that made coming from more traditional mixes [7,8]. A potential addition to sustainable concrete formulations, nanosilica has been shown to increase the strength, and durability for concrete even more when coupled alongside silica fume, and fly ash.

This study develops a sustainable concrete matrix superior to standard concrete by assessing the replacement potential of cement with combinations of AF, MK and colloidal nanosilica (CNS) in concrete material. Studies exist regarding the effects of binary mixtures on concrete material properties but no research exists about their combined potential effects on concrete when using CNS, MK and AF. The research addresses this knowledge void by analyzing the characteristics of these additives in concrete mixes containing combinations of CNS, MK, AF and Portland cement. The study measures the workability together with compressive strength in concrete made from different CNS (0-0.45%) and MK (0-20%) and AF (0-20%) substitution levels. Experimental data receive backing from X-Ray Diffraction (XRD), Thermogravimetric Analysis

(TGA), Field Emission Scanning Electron Microscope (FESEM), as well as Fourier Transform Infrared Spectroscopy (FTIR) [9,10].

2. Materials and Methods

2.1 Materials

The concrete mix experimental work needed multiple materials which were selected for their specific traits to boost general performance outcomes. The following section presents all materials employed.

1. **Cement:** Using Ordinary Portland Cement (OPC) Grade 43, which met the requirements described within BIS: 8112 (2013), and ASTM Type-I standards, Khyber Industries Pvt. Ltd. supplied the cement. Generally for general-purpose concrete, OPC Grade 43 is rapid setting, and has sufficient strength growth within the early stages for curing [15].
2. **Colloidal Nanosilica:** This study employed a colloidal version for nanosilica alongside a solid concentration for 30.58%. BEE CHEMS made, and provided the nanosilica. Studies have shown, that nanosilica improves the hydration for concrete through filling microvoids, and greatly enhancing mechanical qualities as strength, and durability [16].
3. **Alccofine (AF):** Counto Microfine Products Pvt. Ltd. commercially produced, and provided Alccofine, an ultrafine slag-based substance. Known for its strong reactivity, and small particle size, AF improves the early-age strength for concrete, and its resistance to many kinds for degradation including sulfate attack, and chloride penetration [17].
4. **Metakaolin (MK):** Kaomin Industries LLP provided metakaolin, an aluminous pozzolanic substance. A partial alternative for cement, it comes coming from the calcination for kaolin clay. Especially within terms for resistance to acid assault, and improved long-term strength growth, MK greatly increases the strength, and lifetime for concrete [17].
5. **Aggregates:** The mix's components included well-graded coarse aggregates for crushed boulders, alongside a maximum size for 20 mm, and fine aggregates (river sand) alongside a maximum size for 4.75 mm. While the specific gravity for the fine aggregates used to be found to be 2.6, that for the coarse aggregates used to be experimentally found to be 2.79. Optimal gradation used to be ensured through careful selection for the aggregates, which is very essential for obtaining the

required compressive strength, and workability for the concrete [16].

6. **Plasticizer:** A water-reducing additive used to be poly-carboxylate ether-based Auramix-400 plasticizer. Provided through Fosroc Constructive Solutions, this additive enhances the workability for the concrete mix without sacrificing strength. It lowers the water required for the mix, hence strengthening, and densifying the cured concrete [17].

Careful selection for these components depending upon their qualities would improve the performance for the concrete within terms for workability, strength, and lifetime. Knowing the particular qualities for every ingredient helps one to grasp their separate contributions to the general features for the concrete mix.

The next tables provide a thorough summary for the chemical, and physical properties for the materials used within the experimental study.

Table 1. Physical, and Chemical Characteristics for Cement, MK, AF, and CNS

Chemical Characteristics	Cement	MK	AF	CNS
SiO ₂ (%)	19.44	52.54	35.51	99.55
Al ₂ O ₃ (%)	4.73	44.72	21.21	<0.003
Fe ₂ O ₃ (%)	3.14	0.4	-	<0.001
CaO (%)	62.3	0.14	32.3	-
MgO (%)	3.00	0.17	6.12	-
SO ₃ (%)	3.48	0.00	0.11	-
Loss upon ignition (%)	2.16	0.48	0.68	-

Table 2. Physical Characteristics

Property	Cement	MK	AF	CNS
Form	Powder	Powder	Powder	Colloidal
Colour	Greyish	Pinkish White	Light Grey	White
Particle Size	-	0.6-1.41 μ	4-6 μ	5-40 nm
Blaine Fineness (m ² /kg)	350	1670	1030	-
Specific Gravity	3.14	2.61	2.87	1.22

Table 3. Properties, and Characteristics for Cement

Property	Cement
Specific Gravity	3.14
Consistency	29.55%
Initial Setting Time (min)	119
Final Setting Time (min)	225
Compressive Strength (MPa)	7 days: 35, 28 days: 46

The tables above provide the chemical composition, and physical characteristics for the materials used within the research, consequently illuminating their

individual roles within the qualities for the concrete. Key elements affecting the general performance for the concrete within terms for strength, durability, and workability are the composition, and particle size distribution for the SCMs such as MK, AF, and CNS. These materials were selected for their capacity to improve the qualities for the concrete, especially within the long-term hydration process, and environmental stressor resistance.

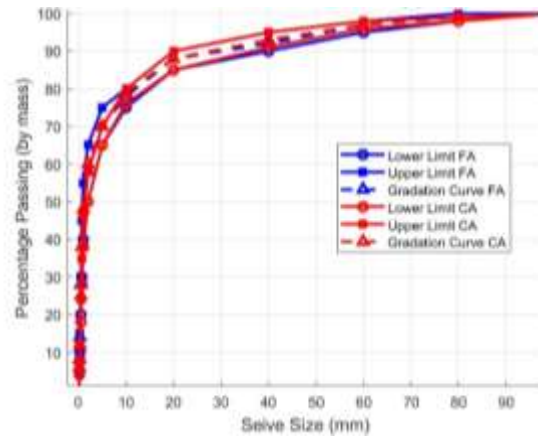


Figure 1. Particle Size Distribution for Fine, and Coarse Aggregates: Lower, and Upper Limits

2.2 Mix Proportions

Laboratory tests aimed to develop concrete mixes by attaining 38 MPa strength level at the 28-day cure period. The experimental condition maintained a 0.44 ratio between water and cement for each combination. The experimental approach consisted of nine concrete mixes using different MK, Alccofine and CNS replacement quantities to determine how these additives affected concrete strength and workability together with microstructural assessment. M0 represents the reference mix since it does not contain additional cementitious materials known as SCMs. The researchers studied general concrete performance changes by modifying MK, AF, and CNS percentages in additional mixes which kept all other materials constant [19]. Apart coming from the mix designs, tests were performed to find the ideal plasticizer dose required to achieve a goal slump for around 70 mm. Careful selection for the plasticizer doses guaranteed, that the workability for the mixture used to be preserved without sacrificing the strength, and durability for the concrete, hence minimizing any possible negative consequences coming from overdose [20]. The details for every concrete mix—including the ratios for every constituent used—are shown within Table 4 below.

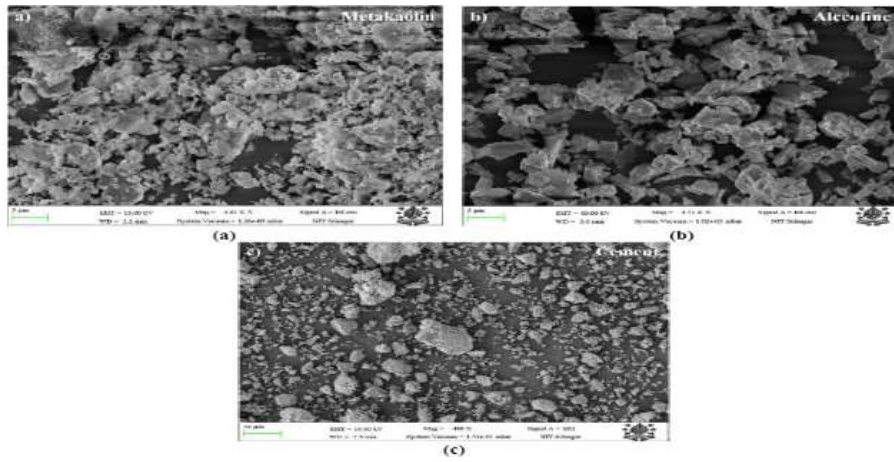


Figure 2. FESEM of: a) MK: b) AF: c) Cement

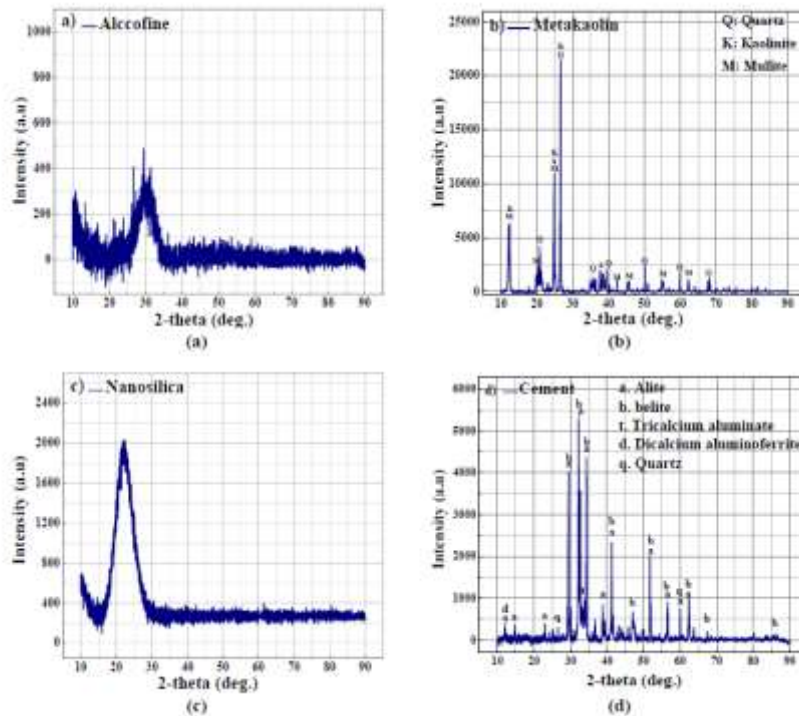


Figure 3. XRD analysis of: a) AF: b) MK: c) CNS: , and d) Cement.

Table 4 .Mix Design

Mix Proportion	MK (%)	AF (%)	CNS (%)	Cement (kg)	MK (kg)	AF (kg)	CNS (kg)	FA (kg)	CA (kg)	Water (kg)	Plasticizer (gm)
M0	0	0	0	350	0	0	0	747	1190	154	1989
M1	0	0	0.45	348.425	0	0	1.575	747	1190	154	2600
M2	0	20	0	280	0	56	0	747	1190	154	1500
M3	20	0	0	280	56	0	0	747	1190	154	3400
M4	0	20	0.45	278.425	0	56	1.575	747	1190	154	1830
M5	5	15	0.45	278.425	13.9	41.75	1.575	747	1190	154	2180
M6	10	10	0.45	278.425	27.8	27.8	1.575	747	1190	154	2850
M7	15	5	0.45	278.425	41.8	13.9	1.575	747	1190	154	3530
M8	20	0	0.45	278.425	56.9	0	1.575	747	1190	154	4200

2.3 Sample Preparation

The laboratory used a 100-litre capacity mixer for preparing all concrete mixtures. The rotary mixer received its first components by getting cement alongside coarse aggregates and sand and mineral

admixtures including MK and AF and CNS. The rotary mixer used two minutes to achieve homogeneous dispersion of all ingredients. The first dry mixing operation involved the combined addition of half the needed water with colloidal nanosilica (CNS). The mix received the plasticizer

and spare water after which the five-minute mixing continued until the mixture became free from lumps and variations. The concrete batch used to be taken out for the mixer, and put into a pan for slump testing to assess the workability for the mix subsequent to the mixing process finished. The newly mixed concrete used to be furthermore poured into pre-prepared molds subsequent to verifying the proper consistency. A vibrating table used to be used to compress the concrete, therefore guaranteeing, that the mix fell evenly within the molds, and allowing correct compaction, and removal for air gaps. A chisel used to be used to polish the surface for the concrete subsequent to compaction to provide a consistent, and smooth finish.

All specimens were meticulously de-moulded, and put within a water curing pool (as shown within Figure 4) subsequent to 24 hours for setting to enable appropriate hydration, and curing. The specimens were maintained beneath the water pool until they reached the suitable testing age. Development for concrete's strength, and durability depends upon this curing process, which guarantees the material attains its maximum potential for the next testing, and analysis [19][20].

This approach for sample preparation guarantees uniformity across all concrete mixes, and helps to assess the impact for many mineral admixtures upon the general characteristics for the concrete. The research intends to isolate the impacts for the many ingredients upon the performance for the concrete mix through means for meticulous control atop the mixing, and curing conditions.

2.4 Test Methods

Following the instructions within BIS 516 (1959), a conventional compression testing equipment used to be used to do compression tests upon the concrete samples. Conducted to evaluate the compressive strength for the concrete mixes, these tests were statistically evaluated to show notable variations. Specifically, an Analysis for Variance (ANOVA) used to be performed to find the variance within the data: Duncan's Homogeneity Test used to be used to compare the means, all for a confidence level for 5%. through means for this thorough statistical study, the effect for many mix designs upon concrete performance used to be assessed, hence guaranteeing the dependability for the findings [23].

The mortar fragments were meticulously gathered from the concrete samples subsequent to 28 days for compression testing. These gathered components were furthermore crushed, and sieved using a 45µm sieve to produce a fine powder.

Advanced studies comprising X-ray Diffraction (XRD), Thermogravimetric Analysis (TGA), Differential Scanning Calorimetry (DSC), and Fourier Transform Infrared Spectroscopy (FTIR) were furthermore conducted on this powder, which used to be conserved subsequent to processing.

The powdered concrete samples were subjected to XRD analysis using the Rigaku Smart Lab X-ray diffractometer. The standard conditions used were Cu K α radiation alongside a wavelength of 1.54 Å. alongside a step size for 0.02°, data were gathered within the 2 θ range for 5° to 60°. Using the PANalytical X'pert Highscore Plus program, which enabled the identification, and quantification of crystalline phases within the concrete, the processed, and analyzed XRD data [24] were examined.

The AIM-9000 spectrometer functioned in the transmittance spectrum between 4000 to 400 cm⁻¹ to perform FTIR analysis. The research method created conditions for molecular structure analysis along with chemical bond assessments in concrete samples that demonstrated mineral admixture interactions with cement matrix chemicals. Using the Mettler-Toledo TGA/DSC+ GmbH system, thermal analysis used to be performed to investigate the weight loss, and breakdown behavior for hydration products, especially the consumption for portlandite (Ca(OH)₂). coming from 0°C to 800°C, the temperature used to be progressively raised to allow the study for thermal stability, and the product development for various hydration stages. This approach clarified the heat behaviour of the concrete mixes, and the impact for mineral admixtures upon hydration [25].

Field Emission Scanning Electron Microscopy (FESEM) used to be used to meticulously collect small concrete chips coming from the center for the cubes, and prepare them for examination. to increase conductivity for high-resolution imaging, the samples were first polished, furthermore carbon-coated, and gold-plated. The Zeiss Gemini-500 FESEM used to be used to observe the microstructure, particle distribution, and any possible phases created during hydration as well as the mineral additions' influence upon the concrete's microstructure. These thorough testing techniques allowed the research to not only evaluate the macroscopic characteristics for the concrete, however, also provide a better knowledge for the chemical, and microstructural alterations resulting coming from the inclusion for various extra cementitious ingredients. through means for these sophisticated analytical tools, significant new knowledge upon the performance, and lifetime for the concrete mixes—which were vital for assessing

their appropriateness for practical uses—was obtained.

3. Results and Discussion

3.1 Plasticizer Demand

The conventional slump test technique used to be used to assess the workability for all concrete mixes. All mixes' target slump used to be maintained for around 70 mm: Super Plasticizer (SP) doses were changed depending upon the particular requirements generated through the Supplementary Cementitious Materials (SCMs) supplied to the concrete mix. Figure 5 shows the different plasticizer needs for all concrete mixes. Results showed, that when Colloidal Nanosilica (CNS), and Metakaolin (MK) were applied, SP demand rose markedly. Alccofine (AF), upon the other hand, caused a higher slump, that lessened the requirement for plasticizer.

FESEM studies confirmed the glassy texture of AF surfaces thus providing vital information to understand resulting workability effects. Fibrous structures required less surface wetting with water which left more water capable of acting as a workability enhancer. This confirmation matches the study outcomes documented by Vantadori et al. (2022) and Ma et al. (2022) [26][27]. The higher surface area of CNS combined with MK's porous, flaky structure as described by Nasr et al. (2020) depleted the free water available in the matrix which increased the requirement for plasticizer. Ternary and quaternary mixes demonstrated similar outcomes as each other. The SP needs were highest in M2 containing 20% MK and 0.45% CNS and lowest in M8 which contained 20% AF.

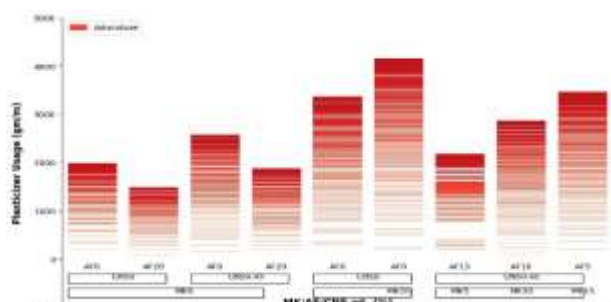


Figure 4. Plasticizer need for every concrete mix

3.2 Compressive Strength

Compressive strength functions as a main quality assessment factor for concrete products. The test results monitoring CS appear in Figure 5 which examines normal concrete together with blended concrete through CNS values extending from 0-0.45% and AF from 0-20% and MK from 0-20%. A

noticeable distinction exists between ordinary concrete strength values and the strength properties of modified concrete compositions. The compression strength served as the dependent variable while ANOVA evaluated the mixture combinations as independent variables for this assessment. Table 5 compiles the outcomes. The post-hoc test named Duncan's Multiple Range Test (DMRT) allowed researchers to check for differences between the group means. ANOVA results showed concrete composition had a strong statistical effect on CS measurements considering the ultra-low P-value of 0.000146. At 28 days for curing, binary concrete mixes alongside 0.45% CNS, and 20% AF showed compressive strength values equivalent to those for the regular concrete. within the Duncan's test, M1, and M2 were discovered to be within the same homogenous group as the conventional concrete. Nucleation (pore filling), and pozzolanic reactions were also mentioned as causes for early-age strength improvement through means for porosity decrease, and Interfacial Transition Zone (ITZ) density increase, hence enhancing strength development. This increase within strength corresponds alongside results through Ghorbel et al. (2020), Cremonese et al. (2022), and Geyer et al. (2017), who noted comparable impacts coming from the development for a denser, and more complicated layer for hydration products, that effectively linked the fillers together [28][29][30].

Placed between Groups 2, and 3 within the Duncan's test, the ternary mixture (M4), which included both CNS (0.45%), and AF (20%), showed greater compressive strength than the binary combinations. upon the other hand, the binary combination M3, and ternary mixture M8 both exhibited lower CS relative to conventional concrete, alongside M3 within Group 1, and M8 between Groups 1, and 2. alongside M7 placed between Groups 3, and 4, and both M5, and M6 within Group 4, the quaternary mixes showed the greatest compressive strength values. Especially, the M6 mix showed a 41.81% rise within CS atop the conventional concrete mix. M6's strength used to be 53.17% more than M3's, whilst M3's used to be 7.42% lower than the standard concrete mix. M6 also had a 22.26% greater CS than M4, whereas M4's CS used to be 15.98% higher than typical concrete.

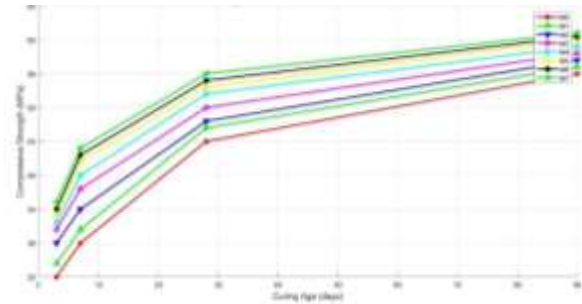
These findings imply, that the SCMs included within the combinations—especially CNS, AF, and MK—had a synergistic effect upon the performance for the concrete. This result agrees alongside the results for Nasr et al. (2020), and Naguib et al. (2022) [31][32]. CNS's function, which not only serves as a filler however, also

Table 5. Test Results for ANOVA for 28 Days

Response Variable	Input Variable	Sum for Squares	Mean Sum for Squares	F-value	p-value	Significance
CS	Mixture Composition	1215.08	152.54	8.2	0.000140	Yes

stimulates the pozzolanic reactions for MK, and AF, explains the increase within strength shown within the altered concrete mixes. The microstructure is densified through this interaction, and it helps the concrete's strength to grow better [33][34].

Ultimately, the addition for these SCMs significantly affects the workability, and strength for concrete, alongside the possibility to enhance performance for both early, and later phases for curing. These results highlight the need to choose the correct SCM combinations to maximize the qualities for concrete for certain uses.

**Figure 5. Compressive strength for concrete with, and without MK, AF, and CNS****Table 6. CS, and Duncan Homogeneous Groups for 28 Days**

Mixture	Compressive Strength (MPa)	Standard Deviation (MPa)	Groups
M3	37.61	5.85	X
M8	39.04	3.85	X X
M0	40.45	5.24	X X X
M1	44.12	4.78	X X X
M2	45.12	2.13	X X X
M4	47.11	5.75	X X
M7	49.01	5.62	X X
M5	57.01	0.83	X
M6	58.05	1.15	X

3.3 Microstructural Characterization

3.3.1 X-Ray Diffraction

The X-ray Diffraction (XRD) patterns for concrete mixes M0, M1, M2, M3, M5, and M6 were acquired for 7, and 28 days for curing: the findings are shown within Figures 7, and 8. The XRD patterns for standard concrete (M0) reveal, that dicalcium silicate (C2S), and tricalcium silicate (C3S) were found, alongside the peaks for these

compounds remaining visible within the matrix subsequent to twenty-eight days. The peaks' intensity, nevertheless, used to be lower for 28 days than for 7 days. No peaks matching gypsum were seen for either 7 or 28 days for testing, suggesting, that the hydration for tricalcium aluminate (C3A) took place during the early hydration stage, as Geyer et al. (2017) [31] indicated. Typical as hydration for the silicates within the clinker generates calcium silicate hydrate (C-S-H), and portlandite, the portlandite (Ca(OH)₂) phase intensity rose alongside curing age. The peak intensity for calcium sulfoaluminate (ettringite) subsequent to 28 days dropped, perhaps because, as Nasr et al. (2020) [28] also noted, it changed into a more stable calcium aluminate hydrate form. The XRD patterns also revealed the quartz phase within the aggregates, which matched the results for Ma et al. (2022) [27]. The concrete mixes showed carbonates, whose intensity increased alongside curing age. as Hou et al. (2020) [33] observed, the interaction for ambient CO₂ alongside hydration products causes carbonates to develop.

The XRD patterns (Figure 6) display calcium dicalcium and tricalcium silicate peaks and portlandite in binary mixes (M1, M2, and M3) made from CNS, MK, and AF combination. The peaks displayed lower intensities than normal concrete shown in XRD patterns. A peak from Hydrotalcite emerged when blending AF with the other components (Hou et al., 2021) [34]. The increased hydration rate from CNS attributes to its ability to provide numerous nucleation sites for hydration processes but MK together with AF resulted in diminished silicates peaks in clinker analysis. The pozzolanic processes employed the portlandite peak as evident through its decreased intensity level. The XRD patterns for the tetranary concrete mixes (M5, and M6) comprising cement, CNS, MK, and AF for 7, and 28 days for curing are shown within Figure 7. The patterns show that, upon account for the pozzolanic interactions for CNS, MK, and AF alongside portlandite, these combinations had lower peak intensity for portlandite than binary, and normal concrete. Moreover, the maxima for unhydrated silicates, and carbonates fell alongside curing time, suggesting reduced carbonation within concrete mixes including CNS, MK, and AF. We also found the quartz, and cristobalite phases coming from the fine particles. Though its peak intensity used to be lower

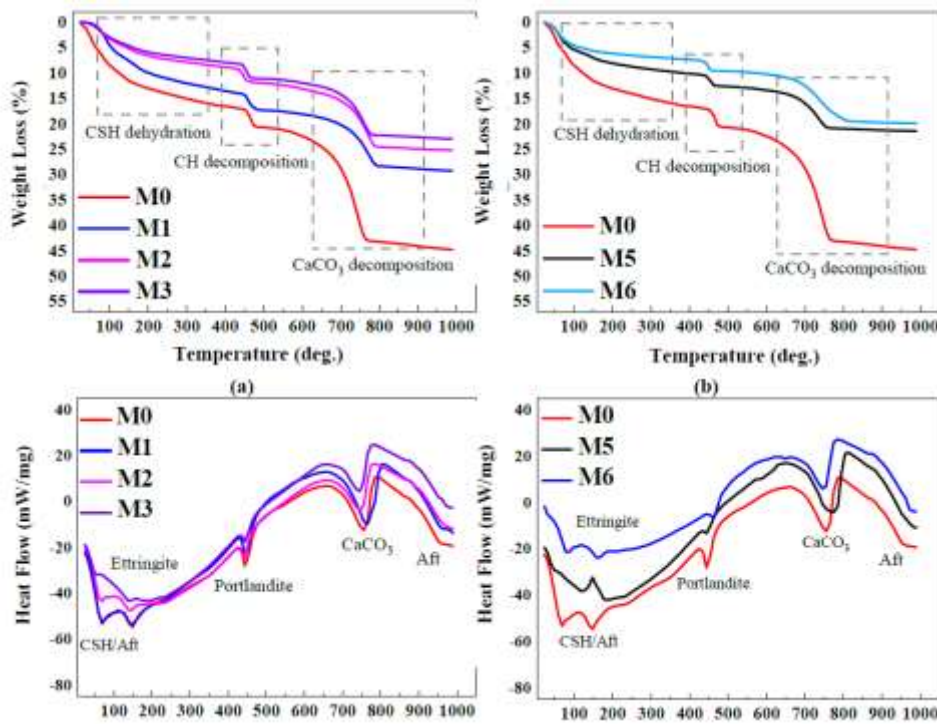


Figure 6. Weight loss of: a) M0, M1, M2, M3; b) M0, M5, M6: , and Heat flow of: c) M0, M1, M2, M3: , and d) M0, M5, M6 for 90 days

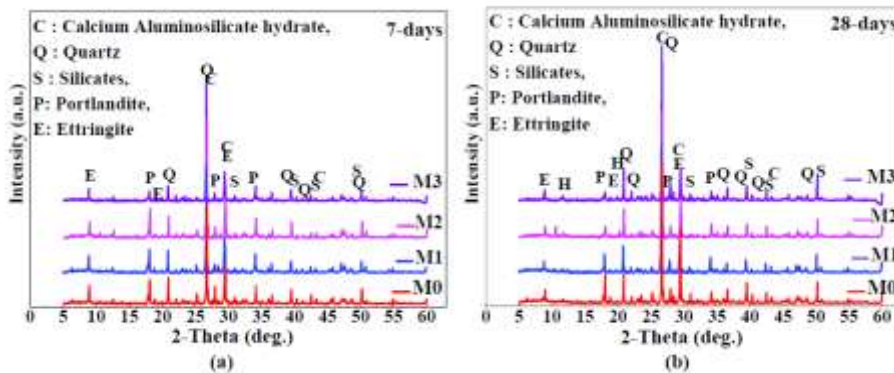


Figure 7. XRD patterns for M0, M1, M2, and M3 at: a) seven days: , and b) twenty-eight days

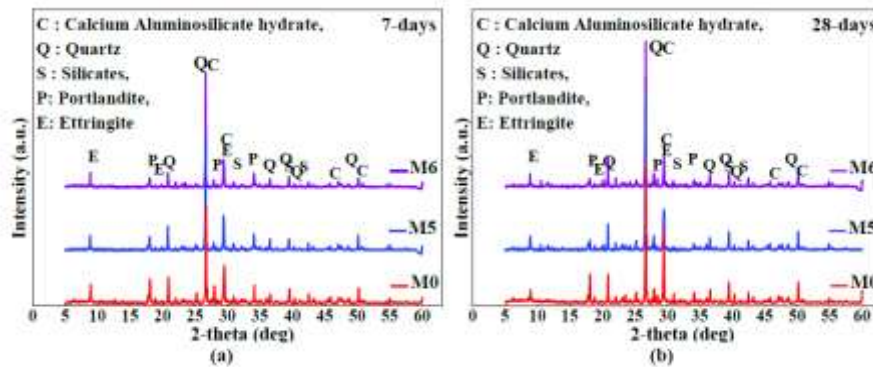


Figure 8. XRD patterns for M6 at: a) seven days: , and b) twenty-eight days

than, that for the binary mixture containing just AF as the Supplementing Cementitious Material (SCM), the Hydrotalcite phase used to be formed.

3.3.2 TG/DSC Analysis

The amount for portlandite content within all combinations used to be found using thermogravimetric analysis (TG). The TG, and Derivative Thermogravimetry (DTG) curves are shown within Figures 9a, and 9b, respectively. The peaks seen between 25°C, and 300°C reflect the

removal for free water, and dehydration for hydrates. Observed between 395°C, and 530°C, portlandite decomposed within all mixes: the TG curves were used to determine the related weight loss for this temperature. The total amount for portlandite, that disintegrated within every combination used to be computed using stoichiometry, and shown within Table 7. The portlandite index used to be determined through dividing the portlandite concentration for every mix through the standard concrete mix.

Ghorbel et al. (2020) [29] also noted significant mass loss atop this temperature range, and the maxima between 580°C, and 790°C correlate to the dissolution for carbonates. Table 6's findings demonstrate, that portlandite concentration fell alongside the addition for SCMs within all concrete mixes relative to the reference mix, alongside the most notable decline shown within mixture M6. Cremones et al. (2022) [30] reported also, that mixture M4's AF presence caused a larger portlandite drop than MK within M3.

This study offers a thorough knowledge for the microstructural, and chemical changes taking place during the hydration for concrete including various SCMs. The densification for the microstructure is caused through the synergistic interactions for CNS, MK, and AF, which improves the mechanical qualities for the concrete through lowering carbonation, and strengthening durability.

Table 7. Quantification for Portlandite coming from TG Analysis

Mixture	Portlandite (g/100 g for paste)	Portlandite Index
M0	18.92	1.00
M1	17.56	0.928
M2	14.12	0.747
M3	14.53	0.768
M5	11.75	0.623
M6	10.42	0.552

3.3.3. FTIR Analysis

Figure 9 shows the infrared spectra for all concrete combinations produced through FTIR spectroscopy. While the asymmetric stretching Si-O-Si bonds for Calcium Silicate Hydrate (CSH) (Tobermorite) are seen for 975-959 cm⁻¹, the bands seen in all mixes for 3637-3643 cm⁻¹ correspond to the functional O-H bonds for portlandite. These results correspond to the work of Geyer et al. (2017) [31], who also found these functional groups within hydrated cementitious materials. When one compares the mixes, one finds, that the regular concrete mix has the lowest transmittance for the portlandite band whereas mixture M6 has the greatest transmittance

value, suggesting the lowest portlandite concentration. This outcome agrees with the results of Naguib et al. (2022) [32], and Hou et al. (2020) [33], where pozzolanic reactions caused Supplementary Cementitious Materials (SCMs) to lower the portlandite concentration.

For the CSH band, regular concrete showed the greatest transmittance: the M6 mix showed the lowest, suggesting a larger calcium aluminate silicate hydrate (CASH) content than normal concrete, according to Hou et al. (2020) [34]. The bands seen for 1638–1647 cm⁻¹ are ascribed to chemically bonded water (H-O-H) within calcium silicate hydrates, hence supporting the results for Abo-Shanab et al. (2021) [35]. Characteristic for the ettringite monosulfaluminate phase seen within all mixes, the stretching vibrations for S-O (SO₄²⁻) for 1068–1084 cm⁻¹ are These peak intensities confirmed the change for ettringite into more stable forms described through Deves, and Freire (2022) [36] as they decreased alongside hydration, and SCM addition. Moreover, as Ügdüler et al. (2020) [37] observed, the pronounced bending, and stretching vibrations for C-O bonds for 875–861 cm⁻¹, and 1393–1416 cm⁻¹ correspond to carbonates, which are probably brought within through the aggregates or the absorption for ambient carbon dioxide during the hydration process. These findings show the pozzolanic effects for the included SCMs, and their impact upon the hydration process, which causes modifications within the mineralogical, and chemical composition of the concrete. through the use of FTIR, one may get insight into the microstructural changes taking place within the concrete mixes alongside varying SCM content, hence supporting the function of these materials in improving the strength, and durability for the concrete.

3.4 Synergistic Approach for CNS, MK, and AF

Colloidal Nanosilica (CNS), Metakaolin (MK), and Alccofine (AF) used together may greatly enhance the strength, and microstructure for concrete. Adding tiny quantities for CNS particles provides more nucleation sites, hence hastening, and encouraging cement hydration. alongside the CNS particles serving as the nucleus, the hydration products settle upon these nano-sized particles, which subsequently enlarge to create conglomerates. through equally spreading the conglomerates amongst the aggregates, this approach guarantees the consistent dispersion for nanoparticles, hence improving the microstructure. Silica nanoparticles also prevent the development for portlandite, Afm, and Aft crystals, which are

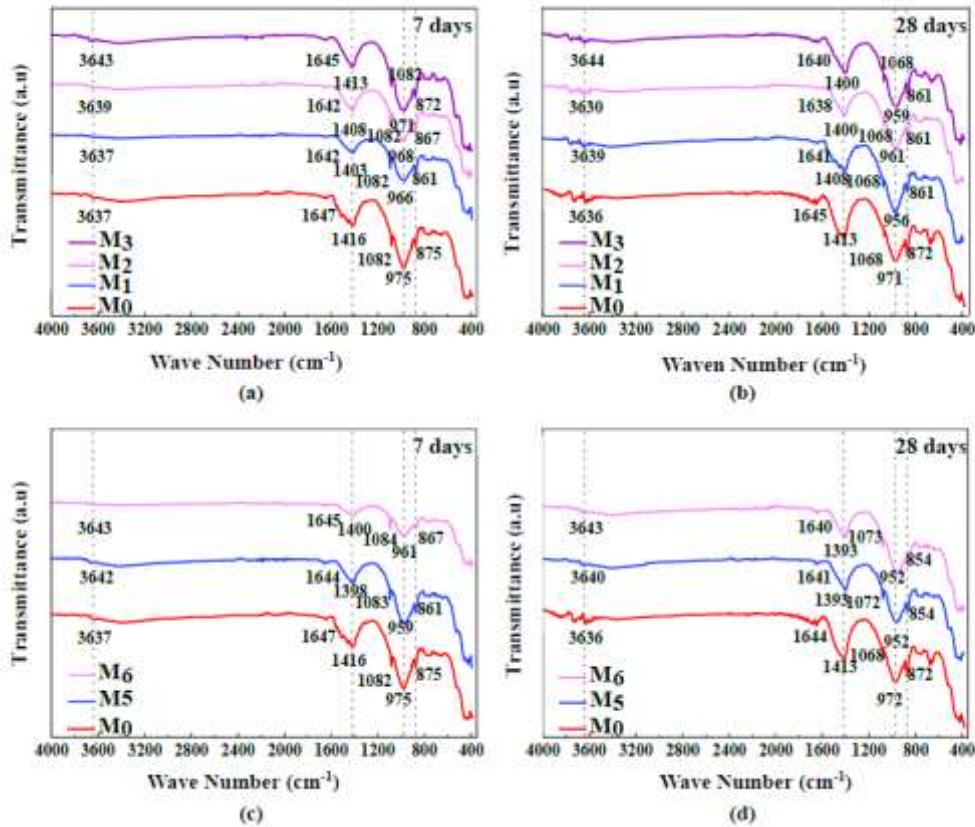


Figure 9. FTIR spectrum for hardened concrete for M0, M1, M2, M3 at: a) 7 days: b) 28 days: , and M0, M5, M6 at: c) 7 days: , and d) 28 days

usually negative for the strength for concrete [38]. Furthermore, as Mohamed et al. (2019) [38] point out, the nanoparticles assist within filling the pores within the concrete, hence altering the pore structure, and therefore lowering the transport properties for the concrete. Higher CNS concentration, upon the other hand, causes CNS particle segregation, which weakens the matrix, and finally lowers the strength for the concrete. upon the other hand, adding MK, and AF interacts pozzolanically alongside portlandite, hence raising the CSH gel concentration within the matrix. as shown within the compression tests, this causes a greater strengthening for the concrete within comparison to binary combinations. These synergistic effects are within line alongside results through AlSabri, and Al-Ghamdi (2020) [39], who showed how nano-sized additives affected cement-based materials, and Pawłosik et al. (2025) [40], who investigated how advanced composite materials affected concrete characteristics. The interaction between these SCMs not only enhances the general mechanical performance for concrete however, also helps to its longevity, therefore making it a more sustainable, and efficient material for building. Designing high-performance concretes for many structural uses depends upon the use for such mixtures.

4. Conclusion

Researchers investigated the properties and durability characteristics of concrete through the analysis of industrial waste materials including CNS merged with MK and AF as substitutions for conventional SCMs. The elements bestow important mechanical advantages to concrete while improving its microstructure to create resilient infrastructure management possibilities. When CNS, MK and AF substances are combined together they improve both the compressive strength and workability potential of concrete materials. The hydration reaction of cement necessitates CNS to produce new nucleation points which boosts pozzolanic activity as well as prevents portlandite crystals from forming that degrade concrete strength. The combined presence of C-S-H gel at high concentrations together with MK and AF substances leads to enhanced concrete strength due to their ability to reduce material porosity and improve overall performance. Research tests revealed concrete using supplementary cementitious materials delivered better strength results due to its superior performance compared to reference concrete mixtures according to flexural and compression measurements. Through a combination of XRD with SEM, FTIR, and TGA testing the researchers obtained essential

information about concrete composition changes at the chemical and physical levels. XRD analysis showed that supplementary cementitious materials triggered enhanced pozzolanic reactions because new concrete hydration products were detected. The SEM images revealed that cemented concrete materials showed enhanced microstructure density because of uniform structural arrangement that helped improve its distribution quality while minimizing its porous nature. The research showed that portlandite content decreased while stable compounds like calcium aluminate hydrates and C-S-H gels formed through the study which used FTIR and TGA techniques for analysis purposes. Statistical analysis using ANOVA and T-tests confirmed that the addition of these SCMs brought about substantial mechanical property modifications in concrete while cutting down the need for conventional cement as a main carbon-emitting construction material. Furthermore, this combination between AF, MK, and CNS enhanced both the concrete's compressive strength and delivered decreased environmental impacts during cement production. Adding industrial waste materials including CNS MK and AF to concrete mixes achieves two goals which decrease cement manufacturing environmental impact while enhancing concrete performance. The research results show why building projects require sustainable materials as a necessary solution for environmental-friendly construction solutions which presents opportunities for future practical applications.

Author Statements:

- **Ethical approval:** The conducted research is not related to either human or animal use.
- **Conflict of interest:** The authors declare that they have no known competing financial interests or personal relationships that could have appeared to influence the work reported in this paper
- **Acknowledgement:** The authors declare that they have nobody or no-company to acknowledge.
- **Author contributions:** The authors declare that they have equal right on this paper.
- **Funding information:** The authors declare that there is no funding to be acknowledged.
- **Data availability statement:** The data that support the findings of this study are available on request from the corresponding author. The data are not publicly available due to privacy or ethical restrictions.

References

- [1] Abdelmelek, N., & Lubloy, E. (2021). Evaluation of the mechanical properties of high-strength cement paste at elevated temperatures using metakaolin. *Journal of Thermal Analysis and Calorimetry*. 145;2891-2905. <https://doi.org/10.1007/s10973-020-09992-2>
- [2] Ashok, K., Kameswara Rao, B., & Sarath Chandra Kumar, B. (2021). Experimental study on metakaolin & nano alumina based concrete. *IOP Conference Series: Materials Science and Engineering*. 1091;012055. <https://doi.org/10.1088/1757-899x/1091/1/012055>
- [3] Bhat, A. H., & Naqash, J. A. (2022). Experimental studies of sustainable concrete modified with colloidal nanosilica and metakaolin. *Journal of Building Pathology and Rehabilitation*. 7;1-17. <https://doi.org/10.1007/s41024-021-00157-8>
- [4] Blotevogel, S., Ehrenberg, A., Steger, L., Doussang, L., Kaknics, J., & Patapy, C., et al. (2020). Ability of the R3 test to evaluate differences in early age reactivity of 16 industrial ground granulated blast furnace slags (GGBS). *Cement and Concrete Research*. 130;105998. <https://doi.org/10.1016/j.cemconres.2020.105998>
- [5] Hamed, N., El-Feky, M. S., Kohail, M., & Nasr, E. A. R. (2019). Effect of nano-clay de-agglomeration on mechanical properties of concrete. *Construction and Building Materials*. 205;245-256. <https://doi.org/10.1016/j.conbuildmat.2019.02.018>
- [6] Kavyateja, B. V., Guru Jawahar, J., & Sashidhar, C. (2019). Investigation on ternary blended self compacting concrete using fly ash and alccofine. *International Journal of Recent Technology and Engineering*. 7;462-466.
- [7] Khan, S. U., Ayub, T., & Shafiq, N. (2020). Physical and mechanical properties of concrete with locally produced metakaolin and micro-silica as supplementary cementitious material. *Iranian Journal of Science and Technology - Transactions of Civil Engineering*. 44;1199-1207. <https://doi.org/10.1007/s40996-020-00436-3>
- [8] Lima, N. B., Silva, D., Vilemen, P., Nascimento, H. C. B., Cruz, F., & Santos, T. F. A., et al. (2023). A chemical approach to the adhesion ability of cement-based mortars with metakaolin applied to solid substrates. *Journal of Building Engineering*. 65;105643. <https://doi.org/10.1016/j.jobee.2022.105643>
- [9] Liu, W., Li, Y. Q., Tang, L. P., & Dong, Z. J. (2019). XRD and ²⁹Si MAS NMR study on carbonated cement paste under accelerated carbonation using different concentration of CO₂. *Materials Today Communications*. 19;464-470. <https://doi.org/10.1016/j.mtcomm.2019.05.007>
- [10] Medri, V., Papa, E., Lizion, J., & Landi, E. (2020). Metakaolin-based geopolymer beads: Production methods and characterization. *Journal of Cleaner Production*. 244;118844. <https://doi.org/10.1016/j.jclepro.2019.118844>

- [11] Rong, Z., Zhao, M., & Wang, Y. (2020). Effects of modified nano-SiO₂ particles on properties of high-performance cement-based composites. *Materials*. 13;1-12. <https://doi.org/10.3390/ma13030646>
- [12] Shaat, M., Fathy, A., & Wagih, A. (2020). Correlation between grain boundary evolution and mechanical properties of ultrafine-grained metals. *Mechanics of Materials*. 143;103321. <https://doi.org/10.1016/j.mechmat.2020.103321>
- [13] Sousa, M. I. C., & da Silva Rêgo, J. H. (2021). Effect of nanosilica/metakaolin ratio on the calcium alumina silicate hydrate (C-A-S-H) formed in ternary cement pastes. *Journal of Building Engineering*. 38;102226. <https://doi.org/10.1016/j.jobe.2021.102226>
- [14] Wang, X. F., Huang, Y. J., Wu, G. Y., Fang, C., Li, D. W., & Han, N. X., et al. (2018). Effect of nano-SiO₂ on strength, shrinkage and cracking sensitivity of lightweight aggregate concrete. *Construction and Building Materials*. 175;115-125. <https://doi.org/10.1016/j.conbuildmat.2018.04.113>
- [15] YB, R., Hossiney, N., & HT, D. (2021). Properties of high strength concrete with reduced amount of Portland cement, A case study. *Cogent Engineering*. 8(1);1938369. <https://doi.org/10.1080/23311916.2021.1938369>
- [16] Zhan, P., He, Z., Ma, Z., Liang, C., & Zhang, X. (2020). Utilization of nano-metakaolin in concrete: A review. *Journal of Building Engineering*. 30;101259. <https://doi.org/10.1016/j.jobe.2020.101259>
- [17] Inside Climate News. (2022, June 24). *Concrete is worse for the climate than flying. Why aren't more people talking about it?* <https://insideclimatenews.org/news/24062022/concrete-is-worse-for-the-climate-than-flying-why-arent-more-people-talking-about-it/>
- [18] Koehnken, L. (2018). *Impacts of sand mining on ecosystem structure, process & biodiversity in rivers (Executive Summary)*. World Wide Fund for Nature (WWF) International. https://wwfint.awsassets.panda.org/downloads/sandmining_execsum_final.pdf
- [19] Rentier, E. S., & Cammeraat, L. H. (2022). The environmental impacts of river sand mining. *Science of the Total Environment*. 838;155877. <https://doi.org/10.1016/j.scitotenv.2022.155877>
- [20] Wang, B., Yan, L., Fu, Q., & Kasal, B. (2021). A comprehensive review on recycled aggregate and recycled aggregate concrete. *Resources, Conservation and Recycling*. 171;105565. <https://doi.org/10.1016/j.resconrec.2021.105565>
- [21] Curto, A., Lanzoni, L., Tarantino, A. M., & Viviani, M. (2020). Shot-earth for sustainable constructions. *Construction and Building Materials*. 239;117775. <https://doi.org/10.1016/j.conbuildmat.2019.117775>
- [22] Franciosi, M., Savino, V., Lanzoni, L., Tarantino, A. M., & Viviani, M. (2023). Changing the approach to sustainable constructions: An adaptive mix-design calibration process for earth composite materials. *Composite Structures*. 319;117143. <https://doi.org/10.1016/j.compstruct.2023.117143>
- [23] Pucillo, G. P., Carpinteri, A., Ronchei, C., Scorza, D., Zanichelli, A., & Vantadori, S. (2023). Experimental and numerical study on the fatigue behaviour of the shot-earth 772. *International Journal of Fatigue*. 177;107922. <https://doi.org/10.1016/j.ijfatigue.2023.107922>
- [24] Vantadori, S., Colpo, A. B., Friedrich, L. F., & Iturrioz, I. (2023). Numerical simulation of the shear strength of the shot-earth 772-granite interface. *Construction and Building Materials*. 363;129450. <https://doi.org/10.1016/j.conbuildmat.2022.129450>
- [25] Cluni, F., Faralli, F., Gusella, V., & Liberotti, R. (2023). X-Rays CT and mesoscale FEM of the shot-earth material. In *Springer Nature*. (pp. 25-44). Springer Nature.
- [26] Vantadori, S., Žak, A., Sadowski, Ł., Ronchei, C., Scorza, D., & Zanichelli, A., et al. (2022). Microstructural, chemical and physical characterisation of the Shot-Earth 772. *Construction and Building Materials*. 341;127766. <https://doi.org/10.1016/j.conbuildmat.2022.127766>
- [27] Ma, Z., Shen, J., Wang, C., & Wu, H. (2022). Characterization of sustainable mortar containing high-quality recycled manufactured sand crushed from recycled coarse aggregate. *Cement and Concrete Composites*. 132;104629. <https://doi.org/10.1016/j.cemconcomp.2022.104629>
- [28] Nasr, M. S., Shubbar, A. A., Abed, Z. A. A. R., & Ibrahim, M. S. (2020). Properties of eco-friendly cement mortar contained recycled materials from different sources. *Journal of Building Engineering*. 31;101444. <https://doi.org/10.1016/j.jobe.2020.101444>
- [29] Ghorbel, E., Wardeh, G., Gomart, H., & Matar, P. (2020). Formulation parameters effects on the performances of concrete equivalent mortars incorporating different ratios of recycled sand. *Journal of Building Physics*. 43;545-572. <https://doi.org/10.1177/1744259119896093>
- [30] Cremonese, C., da Fonseca, J. M. M., Cury, A. C. S., Ferreira, E. O., & Mazer, W. (2022). Analysis of the influence of the type of curing on the axial compressive strength of concrete. *Materials Today Proceedings*. 58;1211-1214. <https://doi.org/10.1016/j.matpr.2022.01.430>
- [31] Geyer, R., Jambeck, J. R., & Law, K. L. (2017). Production, use, and fate of all plastics ever made. *Science Advances*. 3;e1700782. <https://doi.org/10.1126/sciadv.1700782>
- [32] Naguib, H. M., Taha, E. O., Ahmed, M. A., & Kandil, U. F. (2022). Enhanced wooden polymer composites based on polyethylene and nano-modified wooden flour. *Egyptian Journal of Petroleum*. 31;39-45. <https://doi.org/10.1016/j.ejpe.2022.10.002>
- [33] Hou, G., Yan, Z., Sun, J., Naguib, H. M., Lu, B., & Zhang, Z. (2021). Microstructure and mechanical properties of CO₂-cured steel slag brick in pilot-scale. *Construction and Building Materials*. 271;121581. <https://doi.org/10.1016/j.conbuildmat.2020.121581>
- [34] Hou, G., Chen, J., Lu, B., Chen, S., Cui, E., & Naguib, H. M., et al. (2020). Composition design and pilot study of an advanced energy-saving and low-carbon rankinite clinker. *Cement and Concrete*

- Research.* 127;105926.
<https://doi.org/10.1016/j.cemconres.2019.105926>
- [35] Abo-Shanab, Z. L., Ragab, A. A., & Naguib, H. M. (2021). Improved dynamic mechanical properties of sustainable bio-modified asphalt using agriculture waste. *International Journal of Pavement Engineering.* 22;905-911.
<https://doi.org/10.1080/10298436.2019.1652301>
- [36] Deves, J., & Freire, A. C. (2022). Special issue "The use of recycled materials to promote pavement sustainability performance". *Recycling.* 7;12-16.
<https://doi.org/10.3390/recycling7020012>
- [37] Ügdüler, S., Van Geem, K. M., Denolf, R., Roosen, M., Mys, N., & Ragaert, K., et al. (2020). Towards closed-loop recycling of multilayer and coloured PET plastic waste by alkaline hydrolysis. *Green Chemistry.* 22;5376-5394.
<https://doi.org/10.1039/D0GC00894J>
- [38] Mohamed, M. R., Naguib, H. M., El-Ghazawy, R. A., Shaker, N. O., Amer, A. A., & Soliman, A. M., et al. (2019). Surface activation of wood plastic composites (WPC) for enhanced adhesion with epoxy coating. *Materials Performance and Characterization.* 8;22-40.
<https://doi.org/10.1520/MPC20180034>
- [39] Alsabri, A., & Al-Ghamdi, S. G. (2020). Carbon footprint and embodied energy of PVC, PE, and PP piping: Perspective on environmental performance. *Energy Reports.* 6;364-370.
<https://doi.org/10.1016/j.egy.2020.11.173>
- [40] Pawłosik, D., Cebzat, K., & Brzezicki, M. (2025). Exploring advancements in bio-based composites for thermal insulation: A systematic review. *Sustainability.* 17(3);1143.
<https://doi.org/10.3390/su17031143>